DALTON
FULL PAPER

Structural and spectroscopic studies of charge-transfer adducts formed between IBr and thioether crowns

Alexander J. Blake,[a] Francesco A. Devillanova,[b] Alessandra Garau,[b] Francesco Isaia,[b] Vito Lippolis,[a,b] Simon Parsons[c] and Martin Schröder*[a]

[a] *School of Chemistry, The University of Nottingham, University Park, Nottingham, UK NG7 2RD*
[b] *Dipartimento di Chimica e Tecnologie Inorganiche e Metallorganiche, University of Cagliari, Via Ospedale 72, 09124 Cagliari, Italy*
[c] *Department of Chemistry, The University of Edinburgh, West Mains Road, Edinburgh, UK EH9 3JJ*

Received 5th August 1998, Accepted 6th November 1998

Charge-transfer complexes [9]aneS$_3$·2IBr ([9]aneS$_3$ = 1,4,7-trithiacyclononane), [14]aneS$_4$·2IBr **1** ([14]aneS$_4$ = 1,4,8,11-tetrathiacyclotetradecane), [16]aneS$_4$·4IBr **2** ([16]aneS$_4$ = 1,5,9,13-tetrathiacyclohexadecane) and [18]aneS$_6$·2IBr **3** ([18]aneS$_6$ = 1,4,7,10,13,16-hexathiacyclooctadecane) have been synthesized and the single crystal structures of **1**, **2** and **3** determined. The reactions of IBr with [12]aneS$_4$ (1,4,7,10-tetrathiacyclododecane), [15]aneS$_5$ (1,4,7,10,13-pentathiacyclopentadecane) and [24]aneS$_8$ (1,4,7,10,13,16,19,22-octathiacyclotetracosane) have also been examined. All the compounds were prepared by slow evaporation of solutions containing IBr and the appropriate thioether macrocycle in CH_2Cl_2–*n*-hexane. The structure determination of **1** shows the thioether crown lying across a crystallographic inversion centre with two symmetry-related IBr molecules co-ordinated through their iodine atoms to two *exo*-oriented S-donors [S(1)–I(1) 2.678(1), I(1)–Br(1) 2.654(2) Å, S(1)–I(1)–Br(1) 175.53(4)°]. The Br · · · Br contacts between consecutive adduct units form polymeric chains of **1** in the crystal lattice. Compound **2** is the only adduct in the present investigation to have all S-donor atoms of the macrocyclic ligand co-ordinated to IBr molecules [S(1)–I(1) 2.618(2), I(1)–Br(1) 2.7049(11), S(5)–I(5) 2.687(2), I(5)–Br(5) 2.6445(12) Å, S(1)–I(1)–Br(1) 177.65(5), S(5)–I(5)–Br(5) 177.57(5)°]. The [16]aneS$_4$·4IBr units interact with each other through I · · · I and Br · · · I contacts to form ribbons of interconnected molecules of **2** which propagate along the *ab* face diagonals of the unit cell. Compound **3** shows two symmetry-related IBr molecules co-ordinated to the macrocyclic ligand [S(1)–I(1) 2.619(3), I(1)–Br(1) 2.695(2) Å, S(1)–I(1)–Br(1) 175.00(6)°]. Adduct molecules are stacked along the *b* axis and held together by S · · · S interactions between [18]aneS$_6$ units. The structural features and the FT-Raman spectra of the reported IBr adducts are compared with those of the I_2 adducts obtained from the same ligands.

Introduction

Reactions between dihalogens (I_2, Br_2) and interhalogens (IBr, ICl) and molecules containing Group 15[1,2] and 16[3–10] donors have been the subject of renewed interest in the last few years. A great variety of products with different structural archetypes is observed[11–14] (neutral charge-transfer complexes, polyhalide salts, iodonium salts and hypervalent selenium or sulfur derivatives) depending not only on the acidity and basicity of the acceptor and the donor, respectively, but also on the solvent and the molar ratios of the reactants.

Recently, we have reported the results of our investigation of charge-transfer complexes of I_2 with homoleptic thioether macrocycles, both in CH_2Cl_2 solution and in the solid state.[15–17] While in solution the neutral 1:1 adduct is the predominant species, in the solid state a wide range of unusual structures has been observed for the isolated adducts, and structural trends dependent on the diiodine content have been identified. For example, 1:1 adducts always feature I_2 molecules bridging independent S-donor macrocycles to give infinite chain structures. For charge-transfer complexes having higher diiodine content, two- and three-dimensional architectures comprising I_2 and ligand molecules linked *via* S · · · I and I · · · I secondary interactions are observed in the solid state. Moreover, while small to medium-sized macrocycles ([6]aneS$_2$, [6]aneS$_3$, [9]aneS$_3$, [*n*]aneS$_4$ (*n* = 12, 14 or 16), [15]aneS$_5$) always afford adducts in which the I_2 molecule is *exo*-bound, larger ionophores ([18]aneS$_6$ and [24]aneS$_8$) favour *endo* co-ordination of I_2. Interestingly, for some thioether macrocyclic ligands, regardless of the ligand:I_2 reaction molar ratio used, certain adduct stoichiometries are always isolated; this might reflect a preference in the packing behaviour of the isolated products with the I_2 molecule acting as a glue to order the thioether crowns in the solid state.

As a development of our research in this field we report herein the results obtained by treating IBr, which is a stronger acceptor than I_2, with homoleptic thioether macrocycles. The effects on the solid state organization of the charge-transfer complexes obtained are discussed and the FT-Raman spectra of the isolated products analysed on the basis of their structural features.

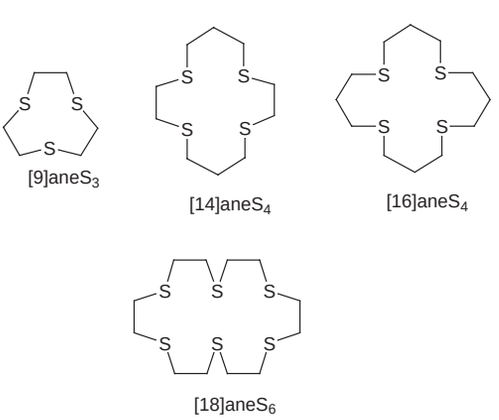

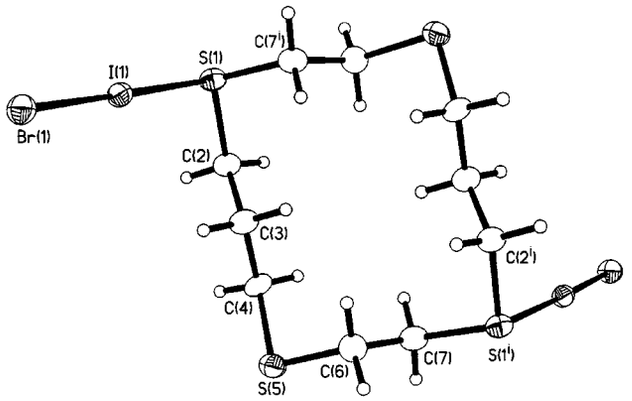

Fig. 1 Single-crystal structure of [14]aneS$_4$·2IBr **1** with the numbering scheme adopted. Displacement ellipsoids are drawn at 50% probability. Symmetry operation: i = $-x + 1$, $-y - 1$, $-z + 2$.

Results and discussion

The reactions between IBr and the cyclic thioether crowns ([9]aneS$_3$, [12]aneS$_4$, [14]aneS$_4$, [16]aneS$_4$, [15]aneS$_5$, [18]aneS$_6$ and [24]aneS$_8$) were performed in an analogous manner to those with I$_2$.[15–17] Solutions of the appropriate macrocycle and IBr (the molar ratios of reactants ranging from 1 : 1 to 1 : 4) in CH_2Cl_2–*n*-hexane (1 : 1 v/v) were allowed to evaporate slowly. In the cases of [12]aneS$_4$ and [24]aneS$_8$ the adducts [12]aneS$_4$·I$_2$[16a] and [24]aneS$_8$·I$_2$,[17] respectively, were isolated in the solid state, as confirmed by microanalytical data and FT-Raman spectroscopy; these two adducts can also be obtained by treating the two macrocyclic ligands directly with I$_2$ in CH_2Cl_2 solution.[16,17] Only oils and lacquers were obtained using [15]aneS$_5$, in accordance with the general tendency of macrocycles containing odd numbers of S-donors to give charge-transfer adducts with I$_2$ which crystallize only with difficulty. Indeed, from the reaction of [9]aneS$_3$ with IBr it was only possible to recover a yellow microcrystalline powder: the formulation [9]aneS$_3$·2IBr was suggested by microanalytical data. Crystals of diffraction quality were grown only for the adducts [14]aneS$_4$·2IBr, [16]aneS$_4$·4IBr and [18]aneS$_6$·2IBr and single-crystal structure determinations were undertaken to elucidate their structural features.

The structure of [14]aneS$_4$·2IBr **1** shows the macrocyclic ligand lying across a crystallographic inversion centre with two symmetry related IBr molecules co-ordinated through the iodine atoms to two S-donors [S(1)–I(1) 2.678(1), I(1)–Br(1) 2.654(2) Å, S(1)–I(1)–Br(1) 175.53(4)°] (Fig. 1, Table 1). The macrocycle adopts a rectangular [3434] conformation as found in the solid state structure of [14]aneS$_4$·I$_2$,[16a] [14]aneS$_4$·2I$_2$,[16a] [14]aneS$_4$·4I$_2$[16b] and free [14]aneS$_4$;[18] all four S-donors are *exo* oriented and lie at the corners of the macrocycle rather than along its edges as found in [14]aneS$_4$·4I$_2$.[16b] The Br · · · Br contacts of 3.330(4) Å between terminal bromine atoms of consecutive [14]aneS$_4$·2IBr units generate chains of charge-transfer adducts parallel to the *ab* face diagonals (shown as thin dashed lines in Fig. 2). Adjacent chains of the same orientation are cross-linked by S · · · I contacts of 3.947(5) Å (shown as dotted lines) to form layers perpendicular to the *c* axis. These layers are cross-linked by S · · · Br contacts of 3.696(4) Å (shown as thick dashed lines in Fig. 2) into a three-dimensional, infinite network. It is interesting that [14]aneS$_4$ is the only thioether macrocycle for which it has been possible to synthesize adducts of both I$_2$ and IBr which have 1 : 2 stoichiometry. With I$_2$ as acceptor, the complexes [14]aneS$_4$·I$_2$[16a] and [14]aneS$_4$·4I$_2$[16b] were also isolated. Moreover, the structure of **1** represents the first example among charge-transfer complexes of thioether crowns with halogens (I$_2$) and interhalogens (IBr) featuring one-dimensional polymeric chains of the type DAAD rather then DAD (D = donor ligand, A = acceptor). Even the analogous adduct [14]aneS$_4$·2I$_2$ exhibits a completly different structure in which adduct molecules are stacked along different directions, linked by S · · · I rather than I · · · I contacts. However, intermolecular I · · · I interactions of 3.639(2) Å have been observed in the structure of [16]aneS$_4$·4I$_2$[16a] where adduct units are linked by I$_2$ · · · I$_2$ bridges into two-dimensional interwoven corrugated sheets.

The compound [16]aneS$_4$·4IBr **2** is the only example in the present investigation where all S-donor atoms of the macro-

Table 1 Selected molecular geometry parameters (distances in Å, angles in °) for [14]aneS$_4$·2IBr **1**

S(1)–I(1)	2.678(1)	I(1)–Br(1)	2.654(2)
S(1)–I(1)–Br(1)	175.53(4)		
C(7^i)–S(1)–C(2)–C(3)	55.2(5)		
S(1)–C(2)–C(3)–C(4)	−176.0(4)		
C(2)–C(3)–C(4)–S(5)	−174.5(4)		
C(3)–C(4)–S(5)–C(6)	−62.9(5)		
C(4)–S(5)–C(6)–C(7)	−69.0(5)		
S(5)–C(6)–C(7)–S(1^i)	−175.7(3)		
C(6)–C(7)–S(1^i)–C(2^i)	64.5(5)		

Symmetry operation: i = $-x + 1$, $-y - 1$, $-z + 2$.

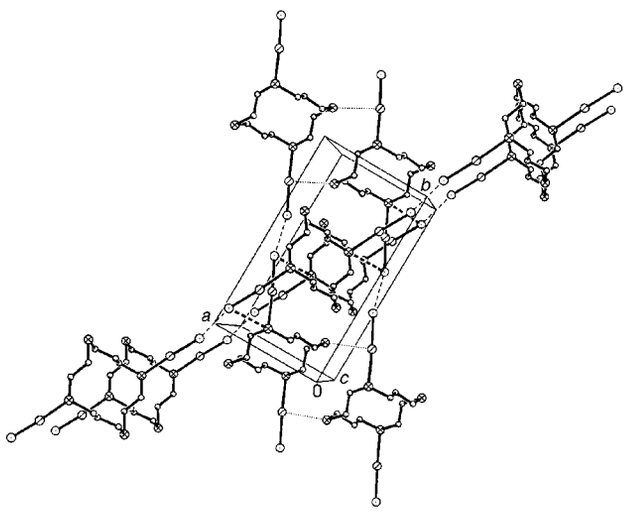

Fig. 2 Partial view approximately along the *c* axis of the crystal packing in [14]aneS$_4$·2IBr **1**. Infinite one-dimensional chains of adduct units run along the *ab* face diagonals and are linked by S · · · I contacts (dotted lines) to form infinite sheets perpendicular to the *c* axis. The S · · · Br contacts (thick dashed lines) generate cross-links among chains in the two distinct orientations.

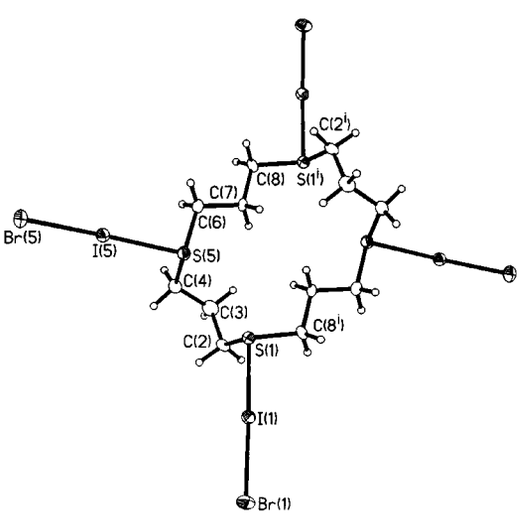

Fig. 3 Single-crystal structure of [16]aneS$_4$·4IBr **2** with the numbering scheme adopted. Displacement ellipsoids are drawn at 50% probability. Symmetry operation: i = $-x + 1$, $-y - 1$, z.

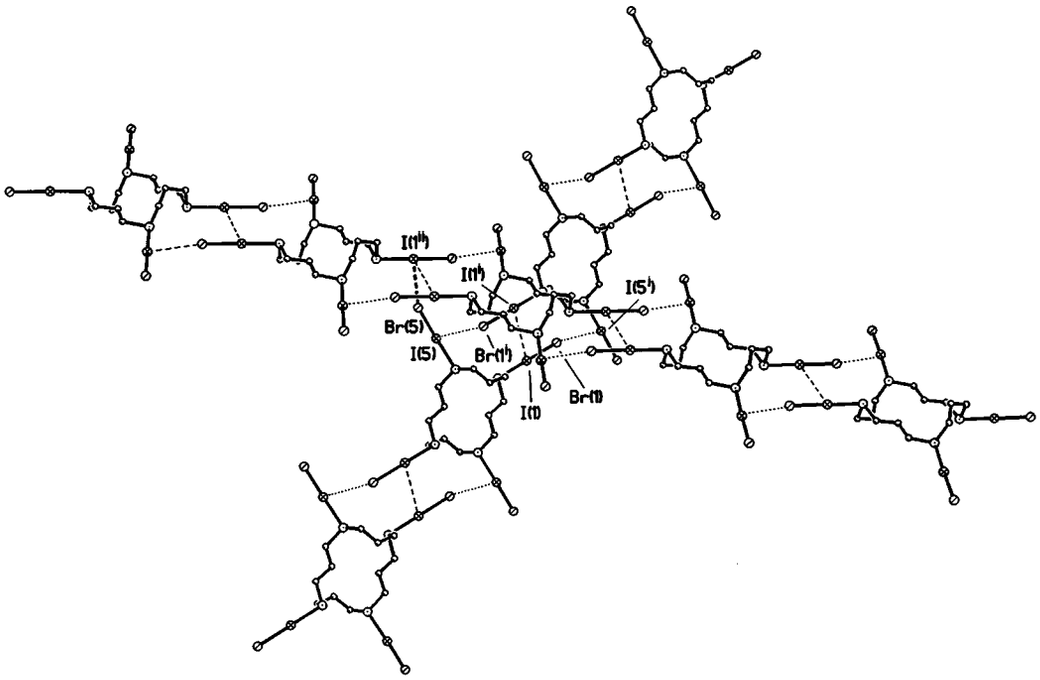

Fig. 4 Partial view approximately along the *c* axis of the crystal packing in [16]aneS$_4$·4IBr **2**. Adduct units are linked by I · · · Br (dotted lines) and I · · · I (dashed lines) contacts to form one-dimensional ribbons that run along the *ab* face diagonals. The I · · · Br interactions (thick dashed lines) link differently oriented ribbons to give a three-dimensional grid.

cyclic ligand are co-ordinated to IBr molecules (Fig. 3, Table 2), a similar situation having been observed only for the adducts [14]aneS$_4$·4I$_2$ [16b] and [16]aneS$_4$·4I$_2$.[16a] While the S(5)–I(5) and I(5)–Br(5) bond distances [2.687(2) and 2.6445(12) Å, respectively] are very similar to the corresponding lengths observed for the S–I–Br moiety in **1**, S(1)–I(1) and I(1)–Br(1) [2.618(2) and 2.7049(11) Å, respectively] are significantly different and clearly indicate a stronger interaction of S(1) with the IBr molecule; the S–I–Br moieties, as expected, are close to linearity [S(1)–I(1)–Br(1) 177.65(5) and S(5)–I(5)–Br(5) 177.57(5)°]. The macrocycle in **2** lies across an inversion centre and adopts an unusual conformation in which 12 out of 16 torsion angles are less than 90°. This is different to either the [3535] conformation of the uncomplexed macrocycle [19] or the [233233] conformation found in the structures of [16]aneS$_4$·I$_2$ and [16]aneS$_4$·4I$_2$.[16a] One S–C–C–C–S linker of the macrocycle lies above and the one opposite it below the plane containing the four S atoms and the remaining two S–C–C–C–S linkers. The pseudo-*endo* orientation of the S atoms in **2** (*i.e.* with the S atoms positioned *along* the sides of the pseudo-rectangle) is very similar to that found in [16]aneS$_4$·4I$_2$ [16a] but different to that observed in either [16]aneS$_4$·I$_2$ [16a] or the free macrocycle,[19] where two *endo*- and two *exo*-oriented S atoms are present, or in the structures of I$_2$ adducts with other tetradentate macrocycles ([12]aneS$_4$, [14]aneS$_4$) [4b,16] where all the S atoms are *exo* oriented (*i.e.* with the S atoms positioned at the corners of the pseudo-rectangle). The packing diagram of **2** (Fig. 4) reveals [16]aneS$_4$·4IBr units interacting with each other through I - - - I (thin dashed lines) and Br · · · I (dotted lines) long-range contacts [I(1) · · · I(1^i) 3.996(1), Br(1) · · · I(5^i) = I(5) · · · Br(1^i) 3.900(1) Å, i = 2 − x, −y, −z] to form ribbons which propagate along the [110] and [1–10] directions. These ribbons are cross-linked by Br · · · I interactions which are shown as thick dashed lines [Br(5) · · · I(1^{ii}) 3.684(1) Å, ii = $-\frac{1}{2} + x$, $\frac{1}{2} - y$, $\frac{1}{2} + z$] to give a "three-dimensional grid". There is a remarkable difference between the structural features of **2** and those of [16]aneS$_4$·4I$_2$ in which molecules of adducts are linked by I$_2$ · · · I$_2$ interactions into infinite chains which are interwoven to form a corrugated bilayer.[16a] Presumably, the more folded conformation adopted by [16]aneS$_4$ in **2** and the different electronic charge distribution within the co-ordinated IBr molecules with respect to the I$_2$ molecules in [16]aneS$_4$·4I$_2$ [16a] are responsible for the different crystal packing in the adducts of I$_2$ and IBr with [16]aneS$_4$.

Table 2 Selected molecular geometry parameters (distances in Å, angles in °) for [16]aneS$_4$·4IBr **2**

S(1)–I(1)	2.618(2)	S(5)–I(5)	2.687(2)
I(1)–Br(1)	2.7049(11)	I(5)–Br(5)	2.6445(12)
S(1)–I(1)–Br(1)	177.65(5)	S(5)–I(5)–Br(5)	177.57(5)
C(8^i)–S(1)–C(2)–C(3)	−88.9(7)		
S(1)–C(2)–C(3)–C(4)	−71.9(9)		
C(2)–C(3)–C(4)–S(5)	78.1(8)		
C(3)–C(4)–S(5)–C(6)	89.1(7)		
C(4)–S(5)–C(6)–C(7)	−86.2(6)		
S(5)–C(6)–C(7)–C(8)	−175.0(6)		
C(6)–C(7)–C(8)–S(1^i)	−179.8(6)		
C(7)–C(8)–S(1^i)–C(2^i)	−81.0(6)		

Symmetry operation: i = $-x + 1$, $-y - 1$, $-z$.

The structure of [18]aneS$_6$·2IBr **3** (Fig. 5, Table 3) shows two IBr molecules co-ordinated to two S atoms in [18]aneS$_6$ with the macrocycle adopting a [22232223] conformation (with 12 out of 18 torsion angles less than 90°) similar to that found in the crystal structure of [18]aneS$_6$·I$_2$,[17] but contrasting with the [2727] and [234234] conformations observed in the structures of [18]aneS$_6$·4I$_2$ [17] and free [18]aneS$_6$,[20] respectively. The S–I and I–Br bond distances [S(1)–I(1) 2.619(3), I(1)–Br(1) 2.695(2) Å] are very similar to those found for the S(1)–I(1)–Br(1) framework in **2** and the S–I–Br angle is approximately linear [175.00(6)°]. The crystal packing (Fig. 6) exhibits adduct molecules stacked along the *b* axis and linked by S · · · S contacts of 3.408(4) Å.

The S–I bond distances in compounds **1**, **2** and **3** [2.618(2)–2.687(1) Å] are significantly shorter than those observed for the I$_2$ adducts of thioether macrocycles [2.741(2)–3.239(1) Å].[16,17] This is in accordance with the polarization of the IBr bond and with the better match in energy between the σ* antibonding orbital of IBr and the lone pairs on the S-donor atom compared to the case of I$_2$ adducts: a stronger S–I bond is then formed in the case of IBr adducts. The IBr bond distance is

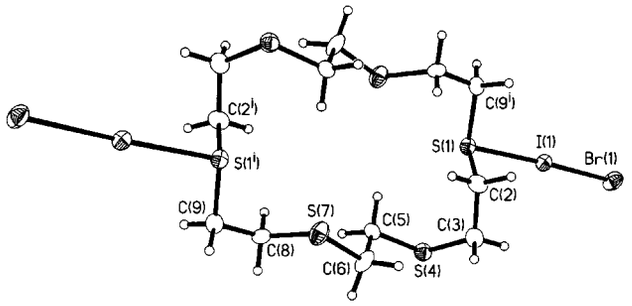

Fig. 5 Single-crystal structure of [18]aneS_4·2IBr **3** with the numbering scheme adopted. Displacement ellipsoids are drawn at 50% probability. Symmetry operation: i = $-x + 3/2, -y + 3/2, -z + 2$.

Table 3 Selected molecular geometry parameters (distances in Å, angles in °) for [18]aneS_6·2IBr **3**

I(1)–S(1)	2.619(3)	I(1)–Br(1)	2.695(2)
S(1)–I(1)–Br(1)	175.00(6)		
$C(9^i)$–S(1)–C(2)–C(3)	−176.9(7)		
S(1)–C(2)–C(3)–S(4)	−48.5(9)		
C(2)–C(3)–S(4)–C(5)	−55.7(8)		
C(3)–S(4)–C(5)–C(6)	−65.7(8)		
S(4)–C(5)–C(6)–S(7)	167.2(6)		
C(5)–C(6)–S(7)–C(8)	65.3(9)		
C(6)–S(7)–C(8)–C(9)	169.1(7)		
S(7)–C(8)–C(9)–$S(1^i)$	57.5(8)		
C(8)–C(9)–$S(1^i)$–$C(2^i)$	67.0(8)		

Symmetry operation: i = $-x + \frac{3}{2}, -y + \frac{3}{2}, -z + 2$.

consequently lengthened with respect to those observed in the solid state [2.521(4)] [21] and in the gas phase for IBr (2.47 Å):[22] donation of electron density from a non-bonding orbital of the S-donors into the σ* LUMO of the IBr molecule lying along the I–Br axis decreases the bond order thus increasing the length of the I–Br bond. A scatter plot of I–X against S–I bond distances (X = I or Br) for solid-state structures of thioether/thiocarbonyl adducts with I_2 and IBr [7,8,16,17,23] is shown as Fig. 7(a). While the relationship between the S–I and I–I bond distances is well defined for I_2 adducts [17,25] (S–I distances lying in the ranges 2.49–2.92, 2.65–2.93 and 3.10–3.22 Å for I_2 molecules co-ordinated to thiocarbonyl S-donors, to thioether S-donors and for bridging I_2 molecules in thioether adducts, respectively), from the few crystallographic data available for neutral IBr adducts it is not yet possible to establish conclusively whether a similar correlation exists between *d*(S–I) and *d*(I–Br).† In order to see whether a generalized relationship can be introduced to describe the structural features of the S–I–X moiety for both I_2 and IBr adducts, we have considered the net increase in the I–X bond distance upon co-ordination Δ*d*(I–X) instead of the absolute *d*(I–X) value [$\Delta d(\text{I–X}) = d(\text{I–X})_{\text{adduct}} - d(\text{I–X})_{\text{IX in gas phase}}$ (X = I or Br)].[8] From the scatter plot of Δ*d*(I–X) against S–I bond distances [Fig. 7(b)] one can see that the available crystallographic data for the neutral adducts of both I_2 and IBr share the same curve. Therefore, Δ*d*(I–X) can be used as a generalized parameter, independent of the nature of the acceptor IX for describing the charge-transfer interaction between sulfur-containing donor molecules and halogens or interhalogens.

In the case of I_2 adducts, another useful tool for investigating the donor–acceptor interaction is based on the I–I bond order (*n*) calculated as a function of the I–I bond distances in the co-ordinated I_2 molecule, according to the equation: $d(\text{I–I}) = d_0 - c\log n$ (d_0 is the I–I bond distance for I_2 in the gas phase, *c* is an empirical constant with a value of 0.85).[26] Depending on the value of *n*, the neutral diiodine adducts have been divided into three main categories:[6c,14a] (1) weak or medium-weak adducts for $n > 0.6$ [d(I–I) < 2.85 Å and Δ*d*(I–X) < 0.18 Å]; (2) strong adducts for $0.4 < n < 0.6$ [2.85 < *d*(I–I) < 3.01 Å and 0.18 < Δ*d*(I–X) < 0.34 Å]; (3) very strong adducts for $n < 0.4$ [*d*(I–I) > 3.01 Å and Δ*d*(I–X) > 0.34 Å] which can be seen as $[\text{D–I}]^+$ cations interacting with an X^- anion (X = I or Br). The use of the parameter Δ*d*(I–X) introduced above allows the same classification to charge-transfer complexes between sulfur containing donor molecules and interhalogens such as IBr and ICl. This places the adducts **1**, **2** and **3**, which have values of Δ*d*(I–Br) ranging from 0.175 to 0.235 Å, on the borderline between the first two categories of adducts if the above ranges of Δ*d*(I–I) defining them are considered roughly valid also for IBr and ICl adducts.

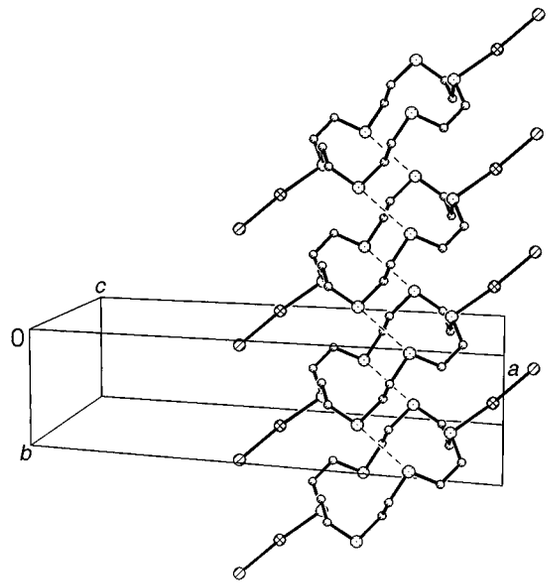

Fig. 6 Stack along the *b* axis of molecules of **3** linked by S···S contacts.

Experimentally, the lengthening of the I–Br bond can also be evaluated by FT-Raman spectroscopy, by measuring the lowering of the *v*(I–Br) stretching frequency as a consequence of adduct formation with respect to the value of 216 cm^{-1} found for solid IBr.[27] In the case of weak and medium-weak I_2 adducts with thioether crowns and thiocarbonyl compounds a linear correlation has been found between the measured *v*(I–I) Raman frequencies and the I–I bond lengths.[17,28] A similar correlation has been proposed for IBr adducts, but this was based on very few experimental data.[27] The FT-Raman spectra in the range 500–50 cm^{-1} for the three structurally characterized IBr adducts with thioether crowns show strong bands at 184 (**1**), 184 and 164 (**2**), and 182 cm^{-1} (**3**) which can be assigned to the *v*(I–Br) stretching vibrations. In the case of **2** the band at the higher wavenumber (184 cm^{-1}) should be assigned to the *v*(I–Br) vibration of the co-ordinated IBr molecule with the shorter I–Br bond distance [I(5)–Br(5)]. A scatter plot of *v*(I–X) against Δ*d*(I–X) (X = I or Br) for I_2 and IBr adducts is shown in Fig. 8. It should be emphasized that many factors influence the observed experimental data: for example, the different accuracy of the reported crystal data or the weak interactions within the crystal lattice involving the S–I–X (X = I or Br) moiety may not be of the same magnitude for all the adducts. This notwithstanding, the slopes of the two correlations, which seem to be linear within the range of the experimental data, are different, reflecting the different nature of the two acceptors (I_2 and IBr). It is of interest that the correlation for I_2 adducts is valid only

† Recently, Husebye and co-workers [11] have shown that for the 3c–4e hypervalent complexes of two-co-ordinated iodine(I) of the type Y–I–X (Y = S, Se or Te; X = I or Br) the reciprocal dependence of *d*(Y–I) on *d*(I–X) is not a simple hyperbola but has a more complicated character.

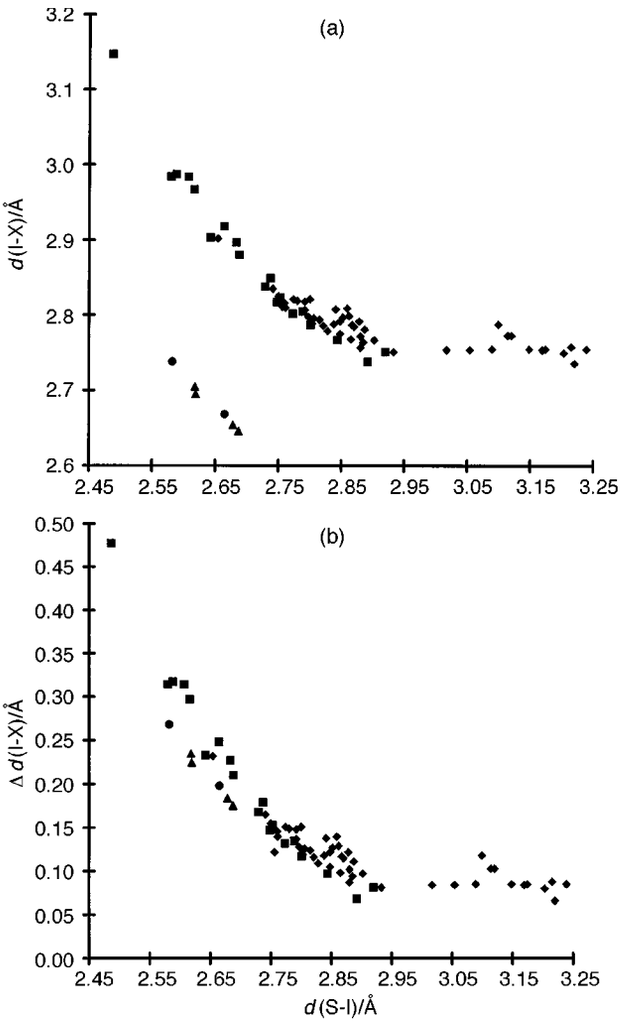

Fig. 7 (a) Scatter plot of d(I–X) against d(S–I); (b) scatter plot of Δd(I–X) against d(S–I) for thiocarbonyl–IX and thioether–IX adducts (X = I or Br) [Δd(I–X) evaluated as the difference between the I–X bond distances measured in the adducts and that in the IX molecule in the gas phase]. (◆) Thiocarbonyl–I_2 adducts;[6,7,16,17] (■) thioether–I_2 adducts;[17] (●) thiocarbonyl–IBr adducts;[8,23] (▲) thioether–IBr adducts from present work and ref. 24.

for weak or medium-weak adducts[28] [d(I–I) < 2.85 Å and Δd(I–I) < 0.18 Å] whereas it appears that the one for IBr adducts can be extended to strong and very strong adducts [0.18 < Δd(I–Br) < 0.34 Å and Δd(I–Br) > 0.34 Å, respectively].‡ Further structural, IR and Raman spectroscopic data are required, particularly for IBr adducts, in order to confirm this linear correlation over a wider range of Δd(I–Br), and also to have better insight into the information the FT-Raman spectroscopy can give on the nature of the charge-transfer interaction of halogens and interhalogens with donor molecules. The adduct [9]aneS_3·2IBr, for which it was not possible to grow crystals suitable for X-ray diffraction studies, shows two main peaks in its FT-Raman spectrum at 197 and 190 cm^{-1}. This suggests the presence of two IBr moieties in the crystal lattice: although both should have slightly elongated I–Br bonds, the presence of two distinct FT-Raman bands implies that these elongations are not the same for each IBr moiety.

The FT-Raman spectra of the adducts of IBr and thioether crowns in CH_2Cl_2 solution have been recorded, and a broad peak in the range 180–195 cm^{-1}, assigned to the ν(I–Br) stretching vibration, is observed for all the adducts. The instability of IBr in CH_2Cl_2 solution has unfortunately prevented the evaluation of the equilibrium constants and the thermodynamic parameters for the formation of the 1 : 1 adducts in solution and it has therefore not been possible to verify the existence of a correlation between ν(I–Br) and ΔH (formation enthalpy of the adduct) for the thioether–IBr 1 : 1 adducts as has been found for the analogous I_2 adducts.[16a,17]

‡ However, the reported ν(I–Br) FT-Raman stretching frequencies for strong IBr adducts would be better assigned to the symmetric stretching of the D–I–Br three body system which would have a major contribution from the ν(I–Br) vibration.[8,27]

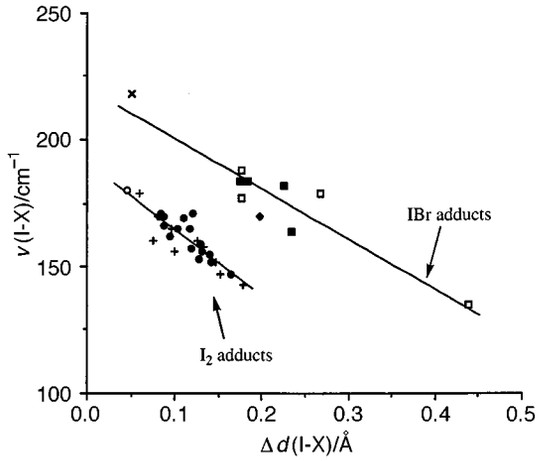

Fig. 8 Scatter plot of ν(I–X) against Δd(I–X) (X = I or Br) for I_2 and IBr adducts with thioether and thiocarbonyl compounds: (×) IBr in the solid state;[27] (○) I_2 in the solid state;[28] (+) thiocarbonyl–I_2 adducts;[6b,28] (●) thioether–I_2 adducts;[17] (■) thioether–IBr adducts (this work); (□) data for IBr adducts from ref. 27; (◆) data from ref. 8. The correlation coefficients from the least-squares best fit are 0.860 and 0.781 for IBr and I_2 adducts, respectively.

Conclusion

We have demonstrated that homoleptic polydentate thioether macrocyclic ligands can interact with IBr molecules to form charge-transfer complexes in a similar manner to I_2. In some cases an I_2 adduct was obtained from the reaction with IBr, demonstrating the tendency of IBr to disproportionate under the experimental conditions. Although the isolated IBr adducts can have the same stoichiometry as their I_2 analogues, their crystal packing is completely different, reflecting the greater acidic character of IBr with respect to I_2. Features common to both groups of adducts are the quasi-linear S–I–X moieties, the elongation of the I–X bond lengths (X = I or Br) compared to those of I_2 and IBr in the vapour and/or solid state, and the close correlation between the S–I and the I–X bond lengths which can be best appreciated by introducing the net increase in the I–X bond distances [Δd(I–X) = $d(\text{I–X})_{\text{adduct}} - d(\text{I–X})_{\text{IX in gas phase}}$] as a generalized parameter, independent of the nature of the acceptor IX. The FT-Raman spectra of the IBr adducts agree fairly well with the observed structural features of the S–I–Br system, and a correlation between the ν(I–Br) Raman frequencies and the d(I–Br) bond distances, similar to that found for I_2 adducts, has been more conclusively established.

Experimental

Solid charge-transfer adducts between polythioether crowns (L) and IBr were prepared in 65–74% yield, by slow evaporation of solutions of IBr and the appropriate thioether macrocycle (0.05–0.08 mmol) in CH_2Cl_2–*n*-hexane (10–15 cm^3 1 : 1 v/v) using L : IBr molar ratios ranging from 1 : 1 to 1 : 4.

FT-Raman spectroscopy

FT-Raman spectra were recorded in the range 500–50 cm^{-1} on a Bruker FRS106 Fourier transform spectrometer, operating

Table 4 Crystallographic data for compounds **1**–**3**

	[14]aneS$_4$·2IBr **1**	[16]aneS$_4$·4IBr **2**	[18]aneS$_6$·2IBr **3**
Formula	$C_{10}H_{20}Br_2I_2S_4$	$C_{12}H_{24}Br_4I_4S_4$	$C_{12}H_{24}Br_2I_2S_6$
M	682.12	1123.79	774.29
Crystal system	Monoclinic	Monoclinic	Monoclinic
Space group	$P2_1/c$ (no. 14)	$P2_1/n$ (no. 14)	$C2/c$ (no. 15)
a/Å	7.997(6)	11.095(3)	24.72(2)
b/Å	14.586(13)	8.106(2)	5.881(3)
c/Å	8.506(9)	15.171(4)	16.794(8)
β/°	105.39(11)	90.77	107.75(4)
U/Å^3	957(2)	1364.3(6)	2325(3)
Z	2	2	4
T/K	150(2)	150(2)	150(2)
μ(Mo-Kα)/mm^{-1}	7.885	10.731	6.675
Reflections collected	1878	4741	1521
Unique reflections, R_{int}	1669, 0.0097	2419, 0.0319	1521,—
Absorption correction			
T_{min}, T_{max}	0.040, 0.067	0.084, 0.152	0.376, 0.721
$R1$	0.0348	0.0356	0.0484
$wR2$ (all data)	0.0922	0.0777	0.1351

with a diode-pumped Nd : YAG laser (1064 nm) with a maximum power of 350 mW. The InGaAs detector was operated at room temperature and all spectra were recorded at 4 cm^{-1} resolution. The solid samples were packed into a suitable cell and then fitted into a compartment designed for 180° scattering geometry. No decomposition of the samples was observed during the spectra aquisition. The CH_2Cl_2 solutions on which the FT-Raman spectra were recorded contained IBr and thioether crown in the ratio 0.4 : 1.0, [IBr] = 2.6×10^{-2} mol dm^{-3}. For the FT-Raman spectra the values in parentheses represent the relative intensities of the bands (strongest = 100).

[9]aneS$_3$·2IBr [Found (Calc. for $C_6H_{12}Br_2I_2S_3$): C, 12.20 (12.13); H, 2.15 (2.04); S, 15.80 (16.19)%]: FT-Raman (cm^{-1}) 296(5), 263(9), 234(16), 204(58), 197(100), 190(90) and 114(5.4).

[14]aneS$_4$·2IBr **1** [Found (Calc. for $C_5H_{10}BrIS_2$): C, 17.58 (17.61); H, 2.78 (2.96); S, 18.35 (18.80)%]: FT-Raman (cm^{-1}) 292(9), 243(10.6), 215(12), 198(40), 184(100), 159(11), 135(27) and 98(2).

[16]aneS$_4$·4IBr **2** [Found (Calc. for $C_6H_{12}Br_2I_2S_2$): C, 12.75 (12.83); H, 2.10 (2.15); S, 10.85 (11.41)%]: FT-Raman (cm^{-1}) 295(11.4), 256(43), 224(10), 184(100), 164(86), 104(14) and 86(6).

[18]aneS$_6$·2IBr **3** [Found (Calc. for $C_6H_{12}BrIS_3$): C, 17.88 (18.61); H, 2.77 (3.12); S, 24.22 (24.84)%]: FT-Raman (cm^{-1}) 229(15), 205(26) and 182(100).

Single-crystal structure determination

A summary of the crystal data and refinement parameters for [14]aneS$_4$·2IBr **1**, [16]aneS$_4$·4IBr **2** and [18]aneS$_6$·2IBr **3** is given in Table 4. The crystals were mounted in the cold dinitrogen stream of an Oxford Cryosystems low-temperature device[29] on a Stoë Stadi-4 four-circle diffractometer using ω–2θ scan mode for **1** and **2** and ω–θ for **3**. Data were corrected for Lorentz-polarization effects and absorption corrections were applied by means of ψ scans. The structures were solved by direct methods using SHELXS 86[30] and developed by alternating cycles of least-squares refinement and ΔF synthesis. Refinement was on F^2 using SHELXL 93.[31] All non-H atoms were refined with anisotropic thermal parameters and H atoms were placed at calculated positions and thereafter refined with $U_{iso}(H) = 1.2\ U_{eq}(C)$. For **1**, **2** and **3** the largest residual electron density features (1.30, 0.89, 1.50 e Å^{-3}) lay near the halogen atoms.

CCDC reference number 186/1236.

Acknowledgements

We thank the EPSRC (UK) and the Consiglio Nazionale delle Ricerche (Italy) for financial support.

References

1 F. A. Cotton and P. A. Kibala, *J. Am. Chem. Soc.*, 1987, **109**, 3308; N. Bricklebank, S. M. Godfrey, A. G. Mackie, C. A. McAuliffe and R. G. Pritchard, *J. Chem. Soc., Chem. Commun.*, 1992, 355; S. M. Godfrey, C. A. McAuliffe, R. G. Pritchard and J. M. Sheffield, *J. Chem. Soc., Dalton Trans.*, 1997, 4823; N. Bricklebank, S. M. Godfrey, H. P. Lane, C. A. McAuliffe, R. G. Pritchard and J. M. Moreno, *J. Chem. Soc., Dalton Trans.*, 1995, 3873; M. Arca, F. Cristiani, F. A. Devillanova, A. Garau, F. Isaia, V. Lippolis and G. Verani, *Heteroatom Chem.*, 1997, **8**, 139.

2 P. Deplano, S. M. Godfrey, F. Isaia, C. A. McAuliffe, M. L. Mercuri and E. F. Trogu, *Chem. Ber., Recueil*, 1997, **130**, 299; V. Stenzel, J. Jeske, W.-W. du Mont and P. G. Jones, *Inorg. Chem.*, 1997, **36**, 443; F. Ruthe, W.-W. du Mont and P. G. Jones, *Chem. Commun.*, 1997, 1947.

3 H. Bock, Z. Havlas, A. Rauschenbach, C. Näther and M. Kleine, *J. Chem. Soc., Chem. Commun.*, 1996, 1529.

4 (*a*) A. L. Tipton, M. C. Lonergan, C. L. Stern and D. F. Shriver, *Inorg. Chim. Acta*, 1992, **201**, 23; (*b*) P. K. Backer, S. D. Harris, M. C. Durrant, D. L. Hughes and R. L. Richards, *Acta Crystallogr., Sect. C*, 1995, **51**, 697; (*c*) H. Bock, N. Nagel and A. Seibel, *Liebig. Ann. Recueil*, 1997, 2151; (*d*) M. Arca, F. Cristiani, F. A. Devillanova, A. Garau, F. Isaia, V. Lippolis, G. Verani and F. Demartin, *Polyhedron*, 1997, **16**, 1983.

5 S. M. Godfrey, C. A. McAuliffe, R. G. Pritchard and S. Sarwar, *J. Chem. Soc., Dalton Trans.*, 1997, 1031, 3501.

6 (*a*) F. Cristiani, F. Demartin, F. A. Devillanova, F. Isaia, G. Saba and G. Verani, *J. Chem. Soc., Dalton Trans.*, 1992, 3553; (*b*) F. Cristiani, F. A. Devillanova, F. Isaia, V. Lippolis, G. Verani and F. Demartin, *Polyhedron*, 1995, **14**, 2937; (*c*) F. Bigoli, P. Deplano, M. L. Mercuri, M. A. Pellinghelli, A. Sabatini, E. F. Trogu and A. Vacca, *J. Chem. Soc., Dalton Trans.*, 1996, 3583.

7 D. C. Apperley, N. Bricklebank, S. L. Burns, D. E. Hibbs, M. B. Hursthouse and K. M. A. Malik, *J. Chem. Soc., Dalton Trans.*, 1998, 1289.

8 M. Arca, F. A. Devillanova, A. Garau, F. Isaia, V. Lippolis, G. Verani and F. Demartin, *Z. Anorg. Allg. Chem.*, 1998, **624**, 745.

9 S. M. Godfrey, S. L. Jackson, C. A. McAuliffe and R. G. Pritchard, *J. Chem. Soc., Dalton Trans.*, 1997, 4499.

10 M. D. Rudd, S. V. Lindeman and S. Husebye, *Acta Chem. Scand.*, 1996, **50**, 759.

11 M. D. Rudd, S. V. Lindeman and S. Husebye, *Acta Chem. Scand.*, 1997, **51**, 689.

12 F. Demartin, P. Deplano, F. A. Devillanova, F. Isaia, V. Lippolis and G. Verani, *Inorg. Chem.*, 1993, **32**, 3694.

13 F. Bigoli, M. A. Pellinghelli, P. Deplano, F. A. Devillanova, V. Lippolis, M. L. Mercuri and E. F Trogu, *Gazz. Chim. Ital.*, 1994, **124**, 445; F. Bigoli, P. Deplano, F. A. Devillanova, V. Lippolis, M. L. Mercuri, M. A. Pellinghelli and E. F Trogu, *Eur. J. Inorg. Chem.*, 1998, **1**, 137.

14 (*a*) F. Demartin, F. A. Devillanova, F. Isaia, V. Lippolis and G. Verani, *Inorg. Chim. Acta*, 1997, **255**, 203; (*b*) F. A. Devillanova, P. Deplano, F. Isaia, V. Lippolis, M. L. Mercuri, S. Piludu, G. Verani and F. Demartin, *Polyhedron*, 1998, **17**, 305.

15 A. J. Blake, R. O. Gould, C. Radek and M. Schröder, *J. Chem. Soc., Chem. Commun.*, 1993, 1191; F. Cristiani, F. A. Devillanova,

F. Isaia, V. Lippolis, G. Verani and F. Demartin, *Heteroatom Chem.*, 1993, **4**, 571.
16 (*a*) A. J. Blake, F. Cristiani, F. A. Devillanova, A. Garau, L. M. Gilby, R. O. Gould, F. Isaia, V. Lippolis, S. Parsons, C. Radek and M. Schröder, *J. Chem. Soc.*, *Dalton Trans.*, 1997, 1337; (*b*) A. J. Blake, W.-S. Li, V. Lippolis and M. Schröder, *Acta Crystallogr., Sect. C*, 1997, **53**, 886.
17 A. J. Blake, F. A. Devillanova, A. Garau, L. M. Gilby, R. O. Gould, F. Isaia, V. Lippolis, S. Parsons, C. Radek and M. Schröder, *J. Chem. Soc.*, *Dalton Trans.*, 1998, 2037.
18 R. E. DeSimone and M. D. Glick, *J. Am. Chem. Soc.*, 1976, **98**, 762.
19 A. J. Blake, R. O. Gould, M. A. Halcrow and M. Schröder, *Acta Crystallogr.*, *Sect B*, 1993, **49**, 773.
20 R. E. Wolf Jr., J. R. Hartman, J. M. E. Storey, B. M. Foxman and S. R. Cooper, *J. Am. Chem. Soc.*, 1987, **109**, 4328.
21 L. N. Swink and G. B. Carpenter, *Acta Crystallogr.*, *Sect B*, 1968, **24**, 429.
22 A. F. Wells, *Structural Inorganic Chemistry*, Clarendon Press, Oxford, 5th edn., 1984.
23 F. Cristiani, F. A. Devillanova, A. Diaz, F. Isaia, V. Lippolis, G. Verani and F. Demartin, *Synthesis and Methodologies in Inorganic Chemistry*, *New Compounds and Materials*, eds. S. Daolio, E. Tondello and P. A. Vigato, Litografia, Padova, 1995, vol. 5, p. 478.
24 C. Knobler, C. Baker, H. Hope and J. D. McCullough, *Inorg. Chem.*, 1971, **10**, 697.
25 F. H. Herbstein and W. Schwotzer, *J. Am. Chem. Soc.*, 1984, **106**, 2367.
26 L. Pauling, in *The Nature of the Chemical Bond*, 3rd edn., Cornell University Press, Ithaca, New York, 1960; H. G. Bürgi, *Angew. Chem.*, *Int. Ed. Engl.*, 1975, **14**, 460.
27 F. Cristiani, F. Demartin, F. A. Devillanova, F. Isaia, V. Lippolis and G. Verani, *Inorg. Chem.*, 1994, **33**, 6315.
28 P. Deplano, F. A. Devillanova, J. R. Ferraro, F. Isaia, V. Lippolis and M. L. Mercuri, *Appl. Spectrosc.*, 1992, **11**, 1625.
29 J. Cosier and A. M. Glazer, *J. Appl. Crystallogr.*, 1986, **19**, 105.
30 G. M. Sheldrick, SHELXS 86, *Acta Crystallogr.*, *Sect. A*, 1990, **46**, 467.
31 G. M. Sheldrick, SHELXL 93, University of Göttingen, 1993.

Paper 8/06172F